

UC Davis

UC Davis Previously Published Works

Title

Inhibition of acetyl-CoA carboxylase by spirotetramat causes growth arrest and lipid depletion in nematodes

Permalink

<https://escholarship.org/uc/item/9bg0320w>

Journal

Scientific Reports, 10(1)

ISSN

2045-2322

Authors

Gutbrod, Philipp

Gutbrod, Katharina

Nauen, Ralf

et al.

Publication Date

2020

DOI

10.1038/s41598-020-69624-5

Copyright Information

This work is made available under the terms of a Creative Commons Attribution License, available at <https://creativecommons.org/licenses/by/4.0/>

Peer reviewed



OPEN

Inhibition of acetyl-CoA carboxylase by spirotetramat causes growth arrest and lipid depletion in nematodes

Philipp Gutbrod^{1,2}, Katharina Gutbrod², Ralf Nauen³, Abdelnaser Elashry^{1,4}, Shahid Siddique^{1,5}, Jürgen Benting³, Peter Dörmann² & Florian M. W. Grundler¹✉

Plant-parasitic nematodes pose a significant threat to agriculture causing annual yield losses worth more than 100 billion US\$. Nematode control often involves the use of nematicides, but many of them including non-selective fumigants have been phased out, particularly due to ecotoxicological concerns. Thus new control strategies are urgently needed. Spirotetramat (SPT) is used as phloem-mobile systemic insecticide targeting acetyl-CoA carboxylase (ACC) of pest insects and mites upon foliar application. However, in nematodes the mode of action of SPT and its effect on their development have not been studied so far. Our studies revealed that SPT known to be activated *in planta* to SPT-enol acts as a developmental inhibitor of the free-living nematode *Caenorhabditis elegans* and the plant-parasitic nematode *Heterodera schachtii*. Exposure to SPT-enol leads to larval arrest and disruption of the life cycle. Furthermore, SPT-enol inhibits nematode ACC activity, affects storage lipids and fatty acid composition. Silencing of *H. schachtii* ACC by RNAi induced similar phenotypes and thus mimics the effects of SPT-enol, supporting the conclusion that SPT-enol acts on nematodes by inhibiting ACC. Our studies demonstrated that the inhibition of de novo lipid biosynthesis by interfering with nematode ACC is a new nematicidal mode of action addressed by SPT, a well-known systemic insecticide for sucking pest control.

Nematodes are widespread organisms with diverse lifestyles including free-living microbe feeders, predators, and obligate parasites of plants and animals. Although they employ fundamentally different life-history strategies, many developmental characteristics are shared. Nematodes hatch from an egg and under favorable conditions develop through consecutive molts into fertile adults, which can propagate and repeat their lifecycles. *Caenorhabditis elegans*, one of the best-studied model organisms, is a free-living nematode. Plant-parasitic nematodes like root-knot and cyst nematodes, on the other hand, have a significant impact on agricultural yields causing a global annual damage of more than 100 billion US\$¹. However, comparably little is known about their basic biology. *Heterodera schachtii*, a cyst nematode, represents an economically important biotrophic parasite of sugar beet, other Chenopodiaceae and Brassicaceae including the model plant *Arabidopsis thaliana*. Following root invasion, *H. schachtii* induces a feeding site containing a syncytium of cells in the root central cylinder. *Heterodera schachtii* actively feeds from the syncytium that provides all nutrients required for its development. While the nematode develops and grows, the feeding site also enlarges and forms strong sink diverting nutrients away from the plant and providing it to the nematode^{2,3}. After hatching from an egg, vermiform L1 of *C. elegans* and J2 of *H. schachtii* will not develop unless they acquire exogenous nutrients. In *C. elegans*, nutrients derived from feeding on bacteria activate a signaling cascade that promotes its development⁴. Similarly, in *H. schachtii* the development of J2s is initiated after feeding from the previously induced syncytium. This indicates that in both nematodes, developmental initiation is tightly linked to nutrient acquisition.

Control of plant-parasitic nematodes is challenging and often requires complex integrated pest management practices that also involve the use of synthetic nematicidal compounds⁵. However, chemical control of

¹INRES, Molecular Phytomedicine, University of Bonn, Bonn, Germany. ²IMBIO, Molecular Physiology and Biotechnology of Plants, University of Bonn, Bonn, Germany. ³Crop Science Division, Bayer AG, Monheim, Germany. ⁴Strube Research GmbH & Co. KG, Schlansted, Germany. ⁵Dept. of Entomology and Nematology, UC Davis, Davis, USA. ✉email: grundler@uni-bonn.de

nematodes is seen controversial by the public due to the potential damage caused to the environment and non-target organisms. Nevertheless, the search for new nematicides is ongoing^{6,7}. In order to predict any potential risks associated with the use of nematicides it is of essential importance to understand their mode of action and to study their exerted effects.

Spirotetramat (SPT) belongs to the class of cyclic keto-enols and is used as a systemic insecticide in crop protection. Within the plant, SPT is hydrolyzed to the corresponding SPT-enol, the presumed active form of SPT. SPT-enol is transported via the phloem, and therefore distributed throughout the plant. In insects and mites, SPT-enol suppresses fatty acid biosynthesis by inhibiting the action of acetyl-CoA carboxylase (ACC)^{8,9}. More specifically, SPT-enol inhibits the carboxyltransferase partial reaction and shows a competitive mode of inhibition with respect to acetyl-CoA and is uncompetitive with respect to ATP¹⁰. Target identification in insects and mites is further supported by studies on the structurally related keto-enol spiromesifen¹¹ suggesting a common mode of action.

ACC catalyzes the initial and rate-limiting step in fatty acid de novo synthesis synthesizing malonyl-CoA via the carboxylation of acetyl-CoA. Malonyl-CoA is used as a substrate for de novo fatty acid biosynthesis by fatty acid synthase (FAS). Fatty acids produced by FAS may be further elongated by the endoplasmic reticulum-(ER-) localized acyl-CoA elongation enzymes that also require malonyl-CoA. Fatty acids may be desaturated and are eventually assembled into complex lipids. Lipids are vital constituents of cells as they are involved in membrane biogenesis (e.g. phospholipids), energy storage (triacylglycerol) and modulation of growth and development (e.g. glycosylceramides)^{12–15}. ACC activity is highly responsive to the overall energy status of a cell which is in turn regulated by nutritional cues. The signal transduction depends on AMP-activated protein kinase (AMPK) that in times of fasting (high AMP, low ATP, low insulin) keeps ACC phosphorylated and thus inactive. In times of abundant nutrients and a high energy charge (low AMP, high ATP, high insulin) AMPK becomes inactive and the proportion of dephosphorylated ACC increases and more malonyl-CoA is synthesized¹⁶.

ACC activity is crucial for embryonic and post-embryonic development of various organisms highlighting the importance of fatty acid de novo synthesis for development. In line with these findings, developmental defects induced by SPT-enol in insects and mites include incomplete molting and reduced fecundity. Furthermore, inhibitory effects were also described for nematodes^{7,17}. However, the underlying mode of action of SPT on nematodes has not been studied. Therefore, we elucidated the mode of action of SPT on *C. elegans* and *H. schachtii*, i.e. on free-living and parasitic nematodes, both under developing and non-developing conditions.

Results

SPT-enol is not acutely toxic for nematodes. To test for an acute toxic effect of SPT-enol we examined its impact on non-developing stages of nematodes, i.e. *C. elegans* starved L1 and *H. schachtii* J2 larvae. When incubated with SPT-enol, the two nematode species were not differently inactivated during the following time course analysis as compared to the solvent control (Supplemental Figure 1A). When the SPT-enol was removed by washing and nematodes were allowed to feed and grow, larval fate was unaffected (Fig. 1C, Supplemental Figure 1B).

To further induce SPT-enol uptake by *H. schachtii* J2 we stimulated them with octopamine, which has been shown to enhance xenobiotic transfer from the surrounding medium into the nematode¹⁸. Similar to our previous observations, preincubation with octopamine and SPT-enol did not affect nematode development (Supplemental Figure 1C). The findings that SPT-enol neither inactivated nematodes over time nor altered their developmental fate after incubation suggest that SPT-enol is not acutely toxic for larval stages that have not yet initiated development.

SPT-enol inhibits nematode development. Next, we tested if SPT-enol would affect the two nematode species during their development, which starts as soon as nutrients are available. SPT-enol inhibited *C. elegans* development in a concentration dependent manner, causing early arrest at stage L1. At a concentration of 100 μ M or above L1 arrest occurs uniformly (Fig. 1B). In a time course experiment, those early arrested larvae became inactive over time (Fig. 1A). To assess if the arrest was reversible, arrested L1 were washed after 2 days and transferred to nematode growth medium (NGM) plates without SPT-enol. Approximately 10% of those arrested L1 were able to recover and became adults whereas all L1 incubated without food source were able to develop irrespective of the presence of SPT-enol (Fig. 1C).

To study the effect of SPT on developing *H. schachtii*, a host plant, in this case *A. thaliana* is required. Therefore, we first analyzed if SPT is hydrolyzed to SPT-enol and transported basipetally from the leaf to the root. In addition, we addressed the question if this treatment would affect the growth of *A. thaliana*, to exclude phytotoxicity as a possible cause of altered nematode development.

After SPT had been applied onto leaves of *A. thaliana*, SPT-enol could be detected in the roots and in the growth medium of the plants (Supplemental Figure 2). SPT applied at a concentration of 200 mM did not affect shoot and root growth (as determined by measuring fresh weight) of the treated plants (Supplemental Figure 3). Taken together these results suggested that SPT is hydrolyzed to SPT-enol *in planta* and translocated basipetally (leaf-to-root) without causing an apparent harm to the plant. Next, we assessed the development of *H. schachtii* infecting SPT-treated plants. Similar to the effect of SPT-enol on *C. elegans*, development of *H. schachtii* infecting SPT-treated plants was arrested in early stages in a concentration-dependent manner (Fig. 2A). In addition, females that did develop on SPT-treated plants were significantly smaller than control nematodes (Fig. 2B). Interestingly, the feeding sites of these developmentally suppressed females were not significantly smaller than those of control nematodes, indicating that the plant response to the infection was not affected. In contrast, feeding sites of nematodes arrested at an early stage were significantly smaller (Fig. 2A, Supplemental Figure 4). Since the feeding sites were induced and nematodes started development, the effect of SPT-enol seems to be restricted

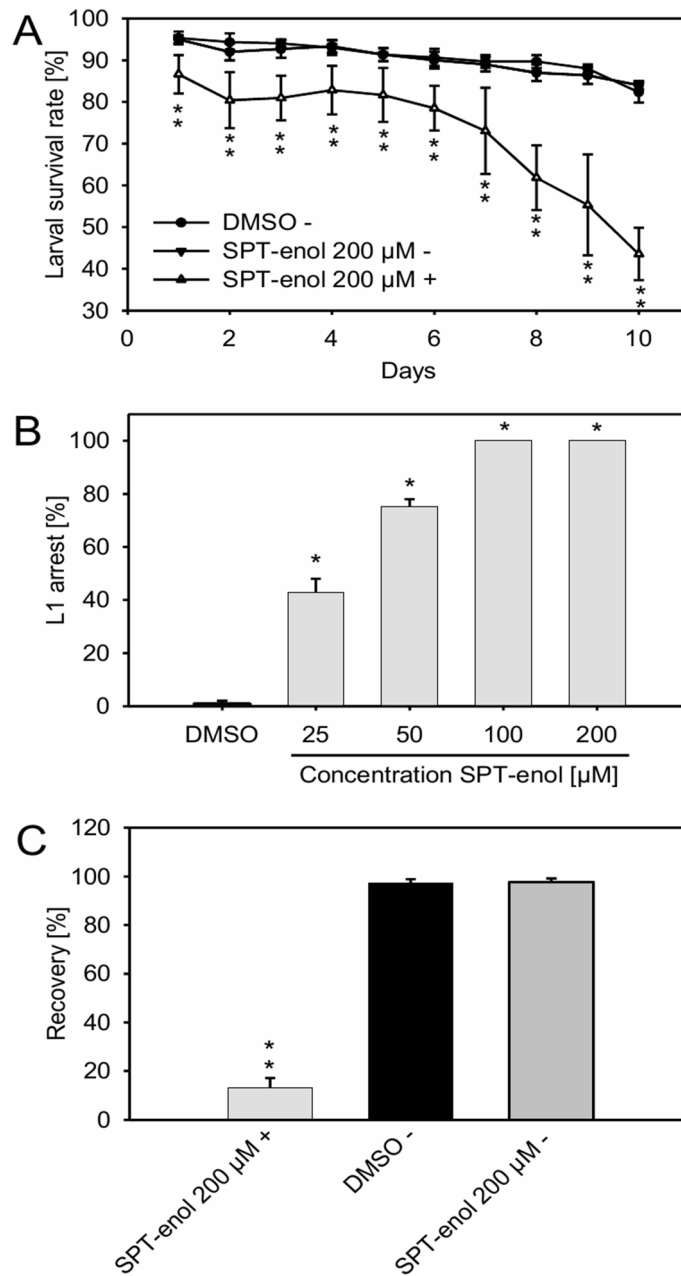
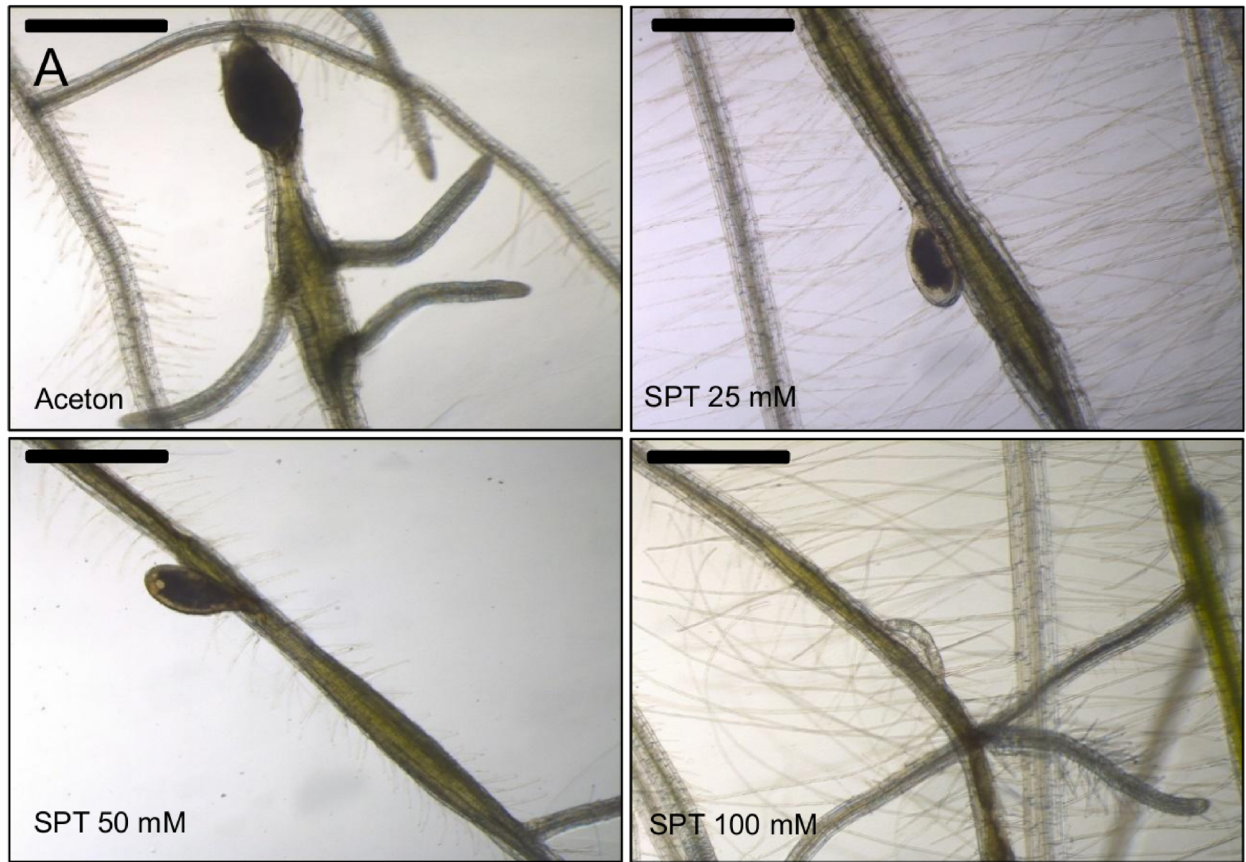


Figure 1. Effect of SPT-enol on *C. elegans* development. **(A)** Time course experiment on survival rate of non-developing and arrested *C. elegans* nematodes. The data are given in average \pm SD ($n=3$). For each time point, Student's t-test was performed for SPT-enol + against DMSO (control) and SPT-enol + against SPT-enol— ($*P<0.001$). **(B)** Concentration-dependent effect of SPT-enol on *C. elegans* larval arrest. The data are given in average \pm SD ($n=3$). For each concentration of SPT-enol, Student's t-test was performed for SPT-enol against DMSO (control) ($*P<0.001$). **(C)** Recovery of non-developing L1 larvae and SPT-enol-arrested larvae of *C. elegans*. The data are given in average \pm SD ($n=3$). Student's t-test was performed for SPT-enol 200 μ M + against DMSO (control) and SPT-enol 200 μ M + against SPT-enol 200 μ M— ($*P<0.001$). In these experiments, (+) and (–) indicate presence or absence of a food source. DMSO plus food source was excluded from the analysis since larvae develop into adults under these conditions.

to nematodes that have initiated development. The data suggest that SPT-enol acts as a developmental inhibitor with a partially reversible effect. Additionally, the juvenile arrest seen in *H. schachtii* seems to be a direct effect of SPT-enol on the nematode rather than indirectly through phytotoxicity.

SPT-enol interferes with lipid metabolism in nematodes by inhibiting ACC. SPT-enol was shown to interfere with lipid metabolism in insects and mites^{8,9}. Given the importance of lipids for development we investigated the effect of SPT-enol on *C. elegans* storage lipids. When treated with SPT-enol, early arrested L1



B

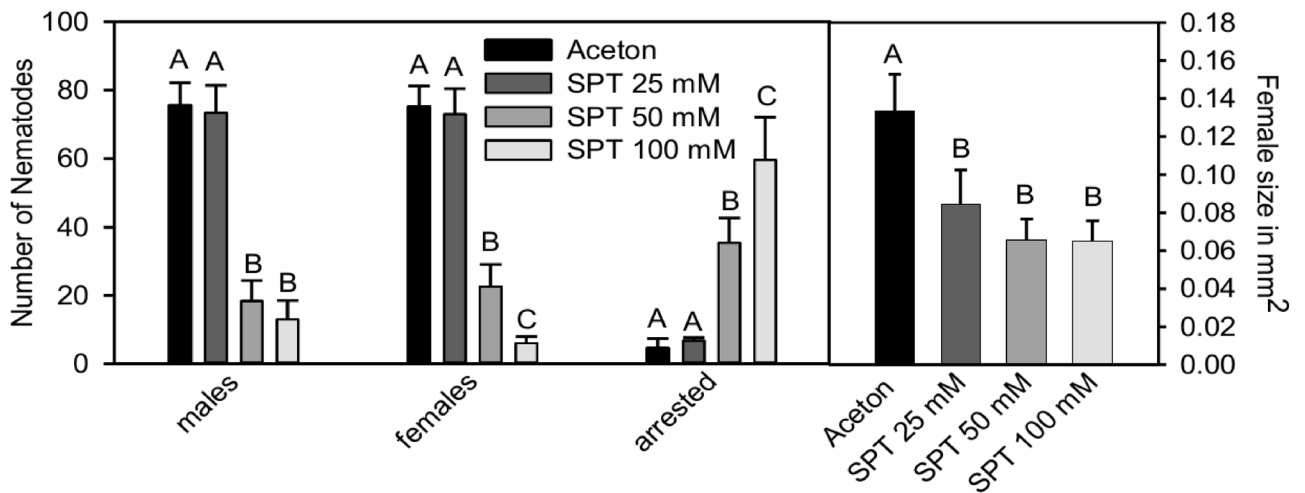


Figure 2. Concentration-dependent effect of foliar application of SPT on *H. schachtii* development. (A) Representative images of *H. schachtii* females in interaction with *A. thaliana* roots after the leaves of the respective plants have been treated with 25 mM, 50 mM and 100 mM SPT. The black bar represents 500 µm. (B) Concentration-dependent effect of foliar SPT application on *H. schachtii*. The data are given in average ± SD. Anova on ranks for males $P=0.002$, Tukey Test, $N=10$; Anova on ranks for females $P<0.001$; Tukey Test, $N=10$; Anova on ranks for arrested $P=0.001$, Tukey Test $N=10$; Anova for sizes $P<0.001$, Tukey Test, $N=30$. Please note that males, females, arrested nematodes and female sizes were analyzed for statistical significance separately.

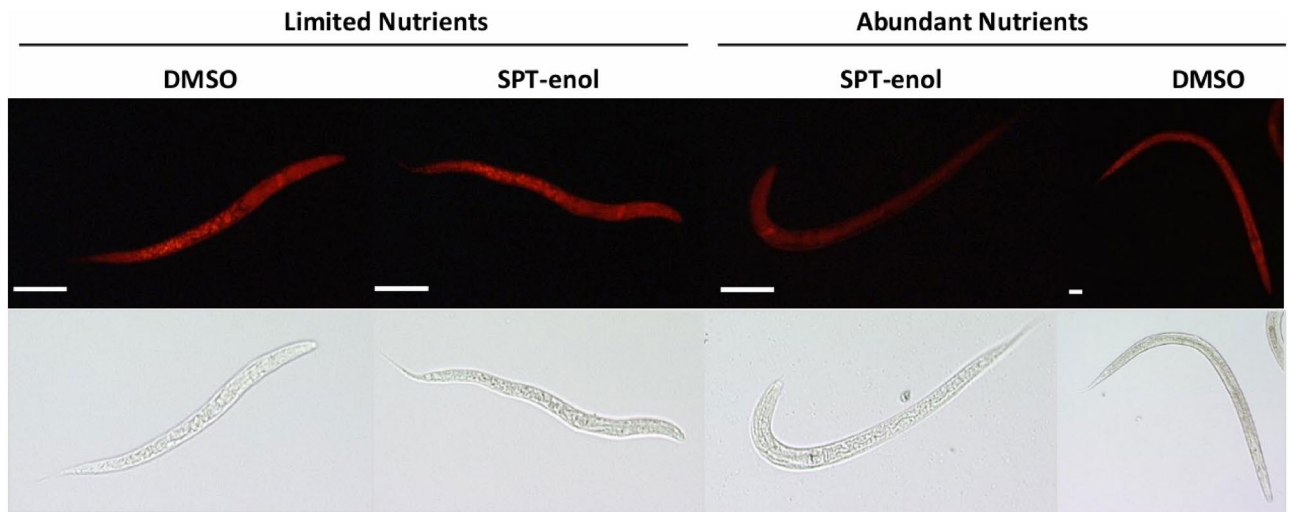


Figure 3. Nile red staining of intestinal lipid droplets of *C. elegans*. Synchronized L1 were incubated in liquid S-medium with 200 μ M SPT or DMSO (control) with and without nutrient source. After 48 h, the nematodes were fixed and stained with Nile red and the number of lipid-depleted nematodes was counted. Only nematodes that were incubated with SPT-enol in the presence of a food source show intestinal lipid droplet depletion ($92.3 \pm 2.5\%$ of total nematodes, average and SD, $n = 3$). Nematodes supplied with food and DMSO start to develop. The white bar represents 50 μ m.

larvae were found to be devoid of intestinal lipid droplets as shown by Nile red staining. In contrast, lipid droplets of L1 incubated for the same time without food source showed similar lipid droplet staining irrespective if SPT-enol was present or not (Fig. 3).

Absence of intestinal lipid droplets may be associated with an altered fatty acid metabolism. Therefore, we analyzed total fatty acids in SPT-enol treated nematodes. We found a reduction of C18 fatty acids while C16 fatty acids were relatively increased (Fig. 4A). To get a more detailed view on storage lipid changes, we determined the triacylglycerol (TAG) content and composition using direct infusion Q-TOF mass spectrometry. We found that SPT-enol treated nematodes had a significantly lower total TAG content as compared to the control (Fig. 4B). The reduction of C18 observed in total fatty acid composition is reflected in changes in TAG composition. When analyzing abundant TAG molecular species it became apparent that 18:1-containing TAG molecules were reduced while TAGs containing 16:1- and 17:cyclo-fatty acids exclusively were unaffected (Fig. 4C). Together this indicates that SPT-enol affects the nematode's storage lipids, by specifically reducing C18-containing TAGs, linking developmental inhibition to fatty acid metabolism. In nematodes, 18:1 is produced via elongation and desaturation of 16:0, while 16:0 can be either taken up by the diet or produced by de novo fatty acid synthesis. Both fatty acid elongation and de novo synthesis require malonyl-CoA. The sole route for malonyl-CoA production in nematodes is carboxylation of acetyl-CoA by ACC. Therefore, we tested whether SPT-enol is able to inhibit ACC activity in vitro. Enzyme assays using radiolabeled sodium bicarbonate showed that *C. elegans* ACC activity is inhibited by SPT-enol with an IC_{50} of 50 μ M (Fig. 4D). This supports the conclusion that the altered fatty acid metabolism in *C. elegans* is linked to ACC inhibition.

Our data show that developmental inhibition observed in both nematode species after SPT-enol treatment is the result of dysfunctional lipid metabolism due to specific inhibition of ACC by SPT-enol.

RNAi mediated silencing of nematode ACC mimics the effect of spirotetramat. To elucidate whether the two nematode species are subject to a common mode of action of SPT-enol on ACC, we searched for the ACC sequence in *H. schachtii*. Using a *H. schachtii* transcriptome data base and the *C. elegans* ACC (POD-2) sequence as query, we retrieved a single contig with a translated ORF of 2024 amino acids. The predicted protein contains all functional domains required for ACC activity and is similar to other nematode ACCs (Supplemental Figure 5A,B). Hence, this implies that we found the *H. schachtii* ortholog of the *C. elegans* ACC (POD-2) and therefore named it *HsACC* (HsPOD-2).

To test if *HsACC* is relevant for the development of *H. schachtii* we investigated the effect of its knock-down upon RNAi. Soaking of J2 in a solution of dsRNA targeted against *HsACC* reduced transcript levels by 90% (Fig. 5B). When allowed to develop on *A. thaliana*, the numbers of males and females were not significantly different, but the developed females were significantly smaller as compared to the control (Fig. 5A,C). To check if transcript reduction was persistent we quantified *HsACC* transcript levels in the developed females 10 days after dsRNA treatment. However, at this stage, *HsACC* transcript levels were no longer significantly different between control and treated females (Fig. 5B).

This suggests that the *HsACC* transcript is involved in *H. schachtii* development. Moreover, its transient knock-down phenocopies the suppressive effect of SPT-enol observed at 25 mM concentrations. Taken together, we conclude that SPT-enol acts on a common nematode target, which is ACC.

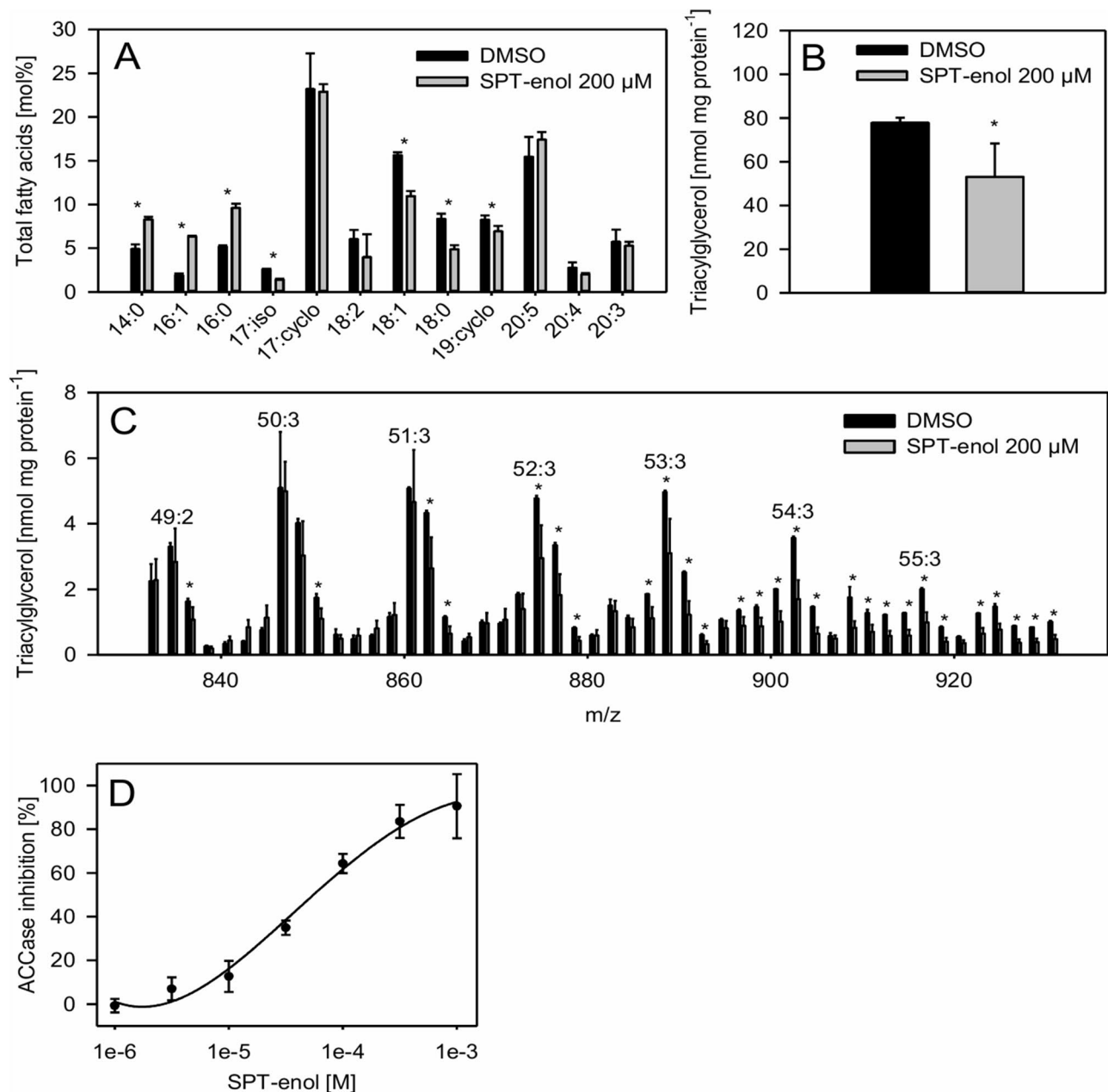


Figure 4. Effect of SPT-enol on fatty acid composition, TAG content and ACC activity of *C. elegans*. **(A)** Total fatty acid composition of *C. elegans* (mol%) after treatment with DMSO (control) or with 200 μM SPT-enol. The data are given in average ± SD (n = 3). Student's t-test was performed (**P* < 0.05). **(B)** Total TAG content of *C. elegans* (nmol mg protein⁻¹) after treatment with DMSO (control) or with 200 μM SPT-enol. The data are given in average ± SD (n = 3). Student's t-test was performed (**P* < 0.05). Representative TAG molecular species are shown in supplemental Table 1. **(C)** Molecular species of TAGs of *C. elegans* (nmol mg protein⁻¹) after treatment with DMSO (control) or with 200 μM SPT-enol. The data are given in average ± SD (n = 3). Student's t-test was performed (**P* < 0.05). **(D)** Relative inhibition of *C. elegans* ACC activity (%) by different concentrations of SPT-enol. The data are given in average ± SD (n = 5).

Discussion

In this article we show that SPT-enol interferes with the development of nematodes by inhibiting ACC. SPT-enol affects the development of two distantly related nematode species, causes lipid droplet depletion and impairs malonyl-CoA dependent fatty acid synthesis. Enzyme inhibition experiments confirmed ACC as the main target of SPT-enol. Furthermore down-regulation of its expression by RNAi mimics the effect of SPT-enol in both *C. elegans* and *H. schachtii*. Together, this strongly supports the scenario that ACC is the target of SPT-enol in nematodes.

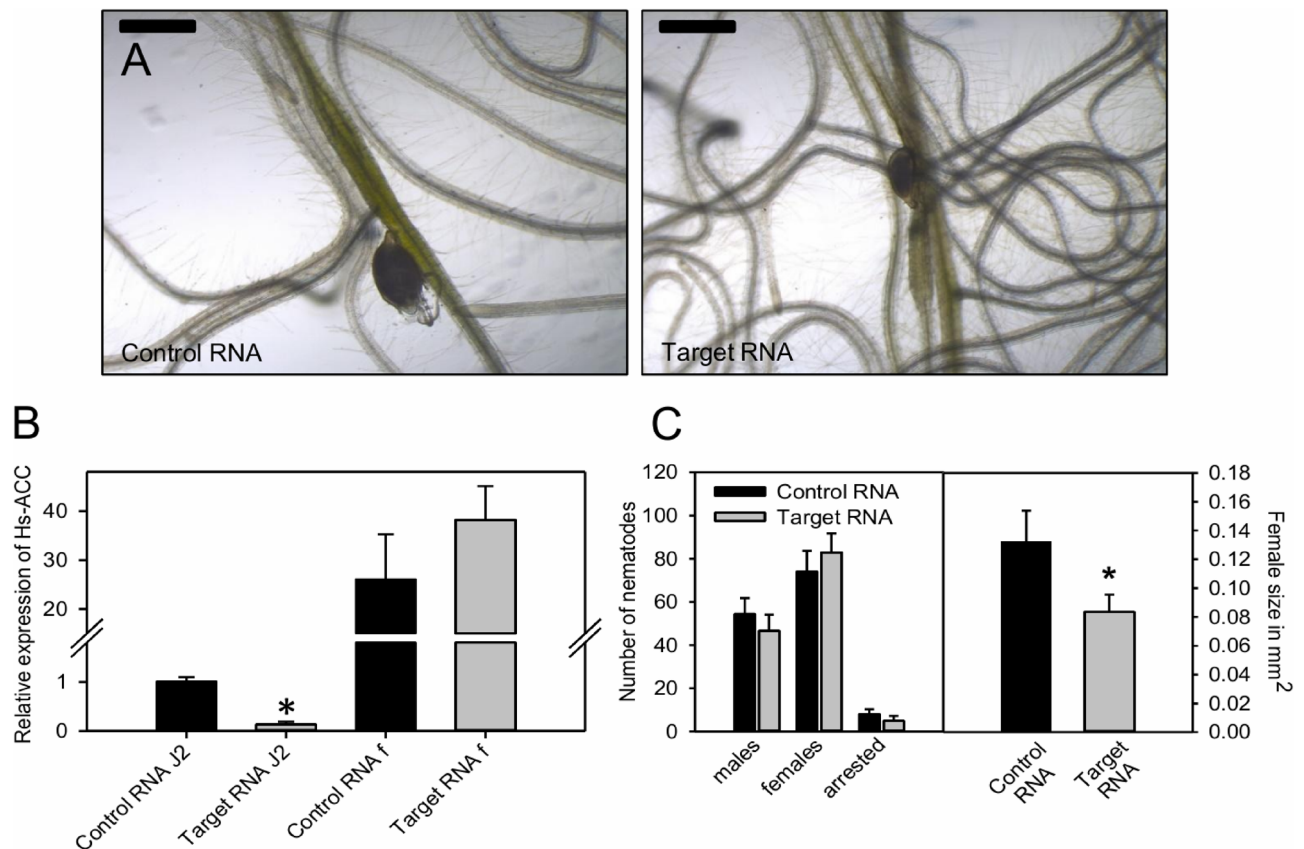


Figure 5. Effect of RNAi against HsACC on *H. schachtii* development. (A) Representative images of *H. schachtii* females in interaction with *A. thaliana* roots after induction of RNAi against HsACC. The bar represents 500 μ m. (B) Relative expression levels of HsACC in *H. schachtii* J2 and in female nematodes after induction of RNAi against HsACC. The data are given in average \pm SD (n = 3). Student's t-test was performed (* P < 0.001). Effect of RNAi against HsACC on total nematode numbers and female size. The data are given in average \pm SD (n = 10 for nematode numbers and n = 30 for female sizes). Student's t-test was performed (* P < 0.001).

ACC catalyzes the initial step in fatty acid biosynthesis converting acetyl-CoA to malonyl-CoA. Malonyl-CoA serves multiple purposes. It supplies C2 units for fatty acid de novo synthesis by fatty acid synthase (FAS), is required for fatty acid elongation and regulates mitochondrial β -oxidation¹⁹. Fatty acids are constituents of structural components of membranes (e.g. phospholipids, sphingolipids), energy stores (triacylglycerol) and are important modulators of development (e.g. phosphoinositides, glycosylceramides)^{15,19}.

In agreement with the important functions of fatty acids, ACC inactivation was found to be lethal in various organisms including nematodes, flies, mice and yeast^{20–23}. Also, polyunsaturated fatty acid (PUFA) synthesis is crucial for development beyond the L1 stage but can be complemented by dietary fatty acids²⁴. In line with these observations, post embryonic knock-down of *C. elegans* POD-2 encoding ACC led to larval arrest²⁵. However, we were not able to rescue the SPT-enol induced developmental arrest in nematodes by dietary supplementation. Similarly ACC defective yeast could also not be rescued by exogenous supply of lipids²⁰. The inability to rescue ACC deficiency pinpointed to a defect in supplying malonyl-CoA for very long chain fatty acid (VLCFA) production which is in turn required for the synthesis of sphingolipids²⁶. Indeed, for *C. elegans* glycosylceramide synthesis is essential for the establishment of cell-polarity and is also required for the activation of TOR signaling, a key activator of development^{14,15}. Furthermore, the inability to synthesize glycosylceramides has been linked to L1 arrest in *C. elegans*²⁷. Therefore, the lack of fatty acid *de-novo* synthesis inhibits the synthesis of specific lipids that are essential for development.

SPT-enol-treated *C. elegans* had lower TAG levels and lacked intestinal lipid droplets when nutrients were present. In addition to its important role in fatty acid synthesis, malonyl-CoA inhibits the action of carnitine palmitoyl transferase (CPT) thereby preventing mitochondrial β -oxidation¹⁶. The absence of malonyl-CoA due to ACC inhibition may explain intestinal lipid droplet depletion under high nutrient conditions. In contrast, lipid droplets in non-developing L1 appeared similar irrespective of the presence of SPT-enol. Interestingly, lowering ACC expression levels by RNAi increases hepatic fat oxidation specifically in the fed state²⁸. In support of these findings, knock-down of ACC by RNAi in feeding *C. elegans* also led to lower storage lipid (TAG) content²⁵. We also observed the inactivation of arrested and lipid depleted *C. elegans* L1 larvae over time. This inactivation may be associated with increased cell death that had been reported in lipid depleted cancer cells due to ACC inhibition²⁹. Thus, lipid depletion seems to drive nematode inactivation possibly by increasing cell death.

Support for a common target of SPT-enol in nematodes is provided by our studies on plant-parasitic *H. schachtii*. SPT does apparently not affect *A. thaliana* growth, SPT-enol is phloem-mobile and the nematodes are arrested in development after feeding site induction. This suggests that SPT acts directly on developing *H. schachtii* rather than through a phytotoxic effect. Both nematode species actively transcribe an ACC mRNA and silencing of *HsACC* by RNAi phenocopies the suppressive effect of SPT-enol on female development. This effect indicates a role for *HsACC* also in *H. schachtii* development and further supports target identification for nematodes.

The IC₅₀ of SPT-enol for insect and mite ACCs in vitro is in the nM range and thus approximately 1,000-fold lower than for nematode ACC^{8–10}. In line with this result, in vivo inhibition of nematode development requires relatively high concentrations of SPT-enol as compared to insects and mites. Therefore, the target affinity of SPT-enol for nematode ACC appears low. This may not be surprising since SPT was developed as an insecticide and the phylogenetic distance and hence ACC sequence differences between nematodes and insects are relatively large. Nevertheless, a formulation of SPT has been reported to reduce cyst nematode populations in wheat¹⁷. This indicates that factors other than the target affinity may ultimately determine the efficacy in the field. Field application of pesticides also poses the risk of causing adverse effects on non-target nematodes and adverse effects cannot be excluded in particular given the broad phylogenetic range of target organisms⁸. Therefore it would be important to assess the effect of SPT field application on the soil inhabiting nematode community.

We found that SPT-enol is not acutely toxic for nematodes but suppresses their development. Non-developing larval stages of *H. schachtii* and *C. elegans* are not inactivated by SPT-enol and their developmental fate is unaffected following SPT-enol removal. Interestingly, SPT-enol inhibition of ACC was shown to be uncompetitive with respect to ATP suggesting that it binds to the enzyme–substrate complex¹⁰. Since ATP content is low under non-developing conditions due to lack of nutrients, SPT-enol may not be able to efficiently bind to the ACC-substrate complex. In contrast, under fed conditions ATP is high and also the effect of an uncompetitive inhibition increases. Thus, the inability to provoke effects in non-developing nematodes may be the result of insufficient ATP levels which are required for SPT-enol to inhibit ACC activity.

In conclusion, this is the first report of ACC as a pharmacological target for nematode control. The findings reported here have significant implications for the treatment of parasitic nematodes in agriculture and may also be translated into novel strategies to fight vertebrate-parasitic nematodes.

Materials and methods

Strains. *Caenorhabditis elegans* Bristol N-2 and *E. coli* OP50 were kindly provided by Prof. Schierenberg, University of Cologne. *C. elegans* was maintained at 20 °C using standard methods and synchronous L1 stages were obtained using alkaline hypochlorite treatment and hatching in M9³⁰.

Drug preparation. For experiments with nematodes in solution, SPT-enol was dissolved in DMSO. For foliar application, SPT was dissolved in acetone.

Liquid culture. Liquid cultures were set up in 24 well plates using 890 µL S-complete, 10 µL active ingredient in DMSO (1% final concentration) and 100 µL M9 buffer containing 250–300 L1s. For starvation experiments bacteria were omitted from the S-complete medium. Liquid cultures were maintained on a shaker with 180 rpm at 20 °C.

Drug recovery assay. Nematodes were collected from liquid cultures, washed twice with M9 and transferred to NGM plates containing *E.coli* OP50. After 3 days developed nematodes were counted.

Nematode fixation and Nile red staining. *Caenorhabditis elegans* were fixed and stained as described previously³¹.

Imaging. Imaging was performed with a binocular microscope (Leica KL200 LED) or with a binocular microscope (Olympus SZX16) equipped with suitable filters to observe Nile red fluorescence.

Lipid quantification. Lipids were extracted from 50 µL mixed-stage worm pellet cultured in S-complete medium with 200 µM SPT-enol or DMSO as control. Triacylglycerol was purified and analyzed as described previously³². Additionally, isolated lipids were transmethylated with 1 N HCl in methanol for 20 min at 80 °C. Fatty acid methyl esters (FAMES) were analyzed by gas chromatography (Agilent 7,890 GC device) coupled to mass spectrometry (GC–MS). FAMES of different chain lengths and degrees of unsaturation were separated on an HP-5MS column using a gradient of 70 °C to 310 °C at 10 °C/min, followed by a hold at 310 °C for 1 min, afterwards the temperature decreases to 70 °C again. Quantification of fatty acids was based on the comparison of the peak area to that of an internal standard, pentadecanoic acid (15:0), which was added in a specified amount (5 µg).

Acetyl-CoA carboxylase assay. Total proteins were extracted from 3 mL of dense *C. elegans* pellet using a protein isolation buffer containing 20 mM HEPES, 150 mM NaCl, 1 mM EDTA, 1 mM DTT, 10% glycerol, 1% protease inhibitor cocktail “Halt” (Thermo Scientific). Determination of ACC activity and inhibition by SPT-enol was performed as described previously¹⁰.

Residue analysis. 10-day-old *A. thaliana* Col-0 plants cultured on 0.2 KNOP plates were treated with 3 μ L 200 mM SPT as described above. After 1, 3 and 10 days, roots and agar were sampled. Roots were thoroughly rinsed with H₂O, blotted dry, weighed, frozen in liquid N₂ and crushed in a Precellys homogenizer (Peqlab Biotechnology). Residues were extracted with 1 mL acetonitrile/H₂O (9:1) and quantification was performed as described previously³³.

Toxicology tests for *H. schachtii*. *H. Heterodera schachtii* was incubated in a solution containing M9 buffer and 500 μ M SPT-enol. The final DMSO concentration was 1%. Non-moving nematodes were counted daily. After 48 h, nematodes in J2 stage were washed with M9 buffer and transferred to 0.2 KNOP plates containing 10-day-old *A. thaliana*.

***H. schachtii* infection assay.** Infection assays were performed on 0.2 KNOP medium as described in Simmons et al.². Per single experiment, 5 plants per petri dish were used. The total numbers of female and male nematodes per plate were counted at 10 DPI and females and feeding site sizes were determined at 14 DPI. Just before nematode inoculation 3 μ L spirotetramat in acetone with the indicated concentrations were applied foliarly onto the largest green leaf. Acetone was allowed to evaporate.

Acetyl-CoA carboxylase transcript identification. A transcript sequence containing a full-length ORF of *H. schachtii* acetyl-CoA carboxylase was identified in a transcriptome database based on sequence similarity to *C. elegans* POD-2 that encodes acetyl-CoA carboxylase. Functional domains were predicted using Pfam (pfam.xfam.org). In order to compare the positions of the predicted functional domains, the HsACC protein sequence was aligned against the *C. elegans* POD-2 sequence (CLC genomics workbench version 6.0).

Sequence analysis. Protein sequences corresponding to full ORF orthologs of *C. elegans* POD-2 were collected from wormbase parasite (parasite.wormbase.org). Domain structures of ACC of *C. elegans* and *H. schachtii* were illustrated using DOG 2.0³⁴. Sequences were aligned using ClustalW. The evolutionary history was inferred using the Neighbor-Joining method³⁵. The optimal tree with the sum of branch length = 4.54642297 is shown. The percentage of replicate trees in which the associated taxa clustered together in the bootstrap test (1,000 replicates) are shown next to the branches³⁶. The tree is drawn to scale, with branch lengths in the same units as those of the evolutionary distances used to infer the phylogenetic tree. The evolutionary distances were computed using the p-distance method³⁷ and are in the units of the number of amino acid differences per site. The analysis involved 60 amino acid sequences. All positions containing gaps and missing data were eliminated. There were a total of 234 positions in the final dataset. Evolutionary analyses were conducted in MEGA5³⁸.

dsRNA synthesis. Using GW primers, a GFP fragment was amplified from pMDC107 and an ACC fragment was amplified from *H. schachtii* (J2s) cDNA and both cloned into pDONR207. dsRNA was synthesized in vitro with T7 overhang primers listed below using MEGAscript[®] T7 Transcription Kit (Ambion, Life technologies) according to the manufacturer protocol.

RNAi of J2s. Induction of RNAi was performed in soaking buffer with 1 μ g/ μ L dsRNA as described¹⁸ with modifications³⁹ for transcript quantification by qPCR. dsRNA of a GFP fragment was used as a control RNA.

Nematode RNA extraction and cDNA synthesis. RNA from nematodes was extracted using the NucleoSpin RNA Plant Kit (Macherey Nagel) according to the supplier's recommendations for low amounts of RNA. Residual DNA was digested using Turbo DNase (Life Technologies) according to the manufacturer's protocol. cDNA was synthesized using the High-Capacity cDNA Reverse Transcription Kit (Applied Biosystems).

qPCR. qPCR was performed using the Fast SYBR Green Master Mix (Life Technologies) on a StepOnePlus System (Life Technologies). qPCR primers for ACC quantification were validated for efficiency and specificity. Actin was used as the reference gene⁴⁰. Relative transcript levels were calculated by the comparative CT method⁴¹ using the StepOnePlus System Software (Life technologies).

Statistics. Statistics were performed with Microsoft Office Excel and SigmaPlot.

Received: 3 February 2020; Accepted: 15 July 2020

Published online: 29 July 2020

References

1. Sasser, J. N. & Freckman, D. W. A world perspective on nematology: the role of the society. *J. Nematol.* **18**, 596 (1986).
2. Sijmons, P. C., Grundler, F. M. W., Mende, N., Burrows, P. R. & Wyss, U. *Arabidopsis thaliana* as a new model host for plant-parasitic nematodes. *Plant J.* **1**, 245–254. <https://doi.org/10.1111/j.1365-3113X.1991.00245.x> (1991).
3. Golinowski, W., Grundler, F. M. W. & Sobczak, M. Changes in the structure of *Arabidopsis thaliana* during female development of the plant-parasitic nematode *Heterodera schachtii*. *Protoplasts* **194**, 103–116. <https://doi.org/10.1007/BF01273172> (1996).
4. Ashrafi, K. Obesity and the regulation of fat metabolism. *WormBook: The Online Review of C. elegans Biology*, 1–20. <https://doi.org/10.1895/wormbook.1.130.1> (2007).

5. Haydock, P. P. J., Woods, S. R., Grove, I. G. & Hare, M. C. Chemical control of nematodes. In *Plant Nematology*, Vol. 2 (eds Perry, R. N. & Moens, M.) 459–479 (CABI, Wallingford, 2013).
6. Faske, T. R. & Hurd, K. Sensitivity of meloidogyne incognita and *Rotylenchulus reniformis* to fluopyram. *J. Nematol.* **47**, 316–321 (2015).
7. Vang, L. E., Opperman, C. H., Schwarz, M. R. & Davis, E. L. Spirotetramat causes an arrest of nematode juvenile development. *Nematology* **18**, 121–131. <https://doi.org/10.1163/15685411-00002948> (2016).
8. Nauen, R., Reckmann, U., Thomzik, J. & Thielert, W. Biological profile of spirotetramat (Movento®)—a new two-way systemic (ambimobile) insecticide against sucking pest species. *Bayer CropSci. J.* **61**, 245–277 (2008).
9. Brück, E. *et al.* Movento®, an innovative ambimobile insecticide for sucking insect pest control in agriculture: biological profile and field performance. *Crop Prot.* **28**, 838–844. <https://doi.org/10.1016/j.cropro.2009.06.015> (2009).
10. Lümmer, P., Khajehali, J., Luther, K. & van Leeuwen, T. The cyclic keto-enol insecticide spirotetramat inhibits insect and spider mite acetyl-CoA carboxylases by interfering with the carboxyltransferase partial reaction. *Insect Biochem. Mol. Biol.* **55**, 1–8. <https://doi.org/10.1016/j.ibmb.2014.09.010> (2014).
11. Karatolos, N. *et al.* Resistance to spiromesifen in *Trialeurodes vaporariorum* is associated with a single amino acid replacement in its target enzyme acetyl-coenzyme A carboxylase. *Insect Mol. Biol.* **21**, 327–334. <https://doi.org/10.1111/j.1365-2583.2012.01136.x> (2012).
12. Watts, J. L. & Browne, J. Genetic dissection of polyunsaturated fatty acid synthesis in *Caenorhabditis elegans*. *Proc. Natl. Acad. Sci. USA* **99**, 5854–5859. <https://doi.org/10.1073/pnas.092064799> (2002).
13. Barber, M. C., Price, N. T. & Travers, M. T. Structure and regulation of acetyl-CoA carboxylase genes of metazoa. *Biochim. Biophys. Acta* **1733**, 1–28. <https://doi.org/10.1016/j.bbali.2004.12.001> (2005).
14. Zhang, H. *et al.* Apicobasal domain identities of expanding tubular membranes depend on glycosphingolipid biosynthesis. *Nat. Cell Biol.* **13**, 1189–1201. <https://doi.org/10.1038/ncb2328> (2011).
15. Zhu, H., Shen, H., Sewell, A. K., Kniazeva, M. & Han, M. A novel sphingolipid-TORC1 pathway critically promotes postembryonic development in *Caenorhabditis elegans*. *eLife* **2**, e00429. <https://doi.org/10.7554/eLife.00429> (2013).
16. Berg, J. M., Tymoczko, J. L. & Stryer, L. Acetyl coenzyme A carboxylase plays a key role in controlling fatty acid metabolism. In *Biochemistry*, Vol. 5 (eds Berg, J. M. *et al.*) (W H Freeman, New York, 2002).
17. Smiley, R. W., Marshall, J. M. & Yan, G. P. Effect of foliarly applied spirotetramat on reproduction of *Heterodera avenae* on wheat roots. *Plant Dis.* **95**, 983–989. <https://doi.org/10.1094/PDIS-01-11-0017> (2011).
18. Urwin, P. E., Lilley, C. J. & Atkinson, H. J. Ingestion of double-stranded RNA by parasitic juvenile cyst nematodes leads to RNA interference. *Mol. Plant Microbe Interact.* **15**, 747–752. <https://doi.org/10.1094/MPMI.2002.15.8.747> (2002).
19. Watts, J. L. Fat synthesis and adiposity regulation in *Caenorhabditis elegans*. *Trends Endocrinol. Metab.* **20**, 58–65. <https://doi.org/10.1016/j.tem.2008.11.002> (2009).
20. Hasslacher, M., Ivessa, A. S., Paltauf, F. & Kohlwein, S. D. Acetyl-CoA carboxylase from yeast is an essential enzyme and is regulated by factors that control phospholipid metabolism. *J. Biol. Chem.* **268**, 10946–10952 (1993).
21. Tagawa, A., Rappleye, C. A. & Aroian, R. V. Pod-2, along with pod-1, defines a new class of genes required for polarity in the early *Caenorhabditis elegans* embryo. *Dev. Biol.* **233**, 412–424. <https://doi.org/10.1006/dbio.2001.0234> (2001).
22. Abu-Elheiga, L. *et al.* Mutant mice lacking acetyl-CoA carboxylase 1 are embryonically lethal. *Proc. Natl. Acad. Sci. USA* **102**, 12011–12016. <https://doi.org/10.1073/pnas.0505714102> (2005).
23. Parvy, J. P. *et al.* *Drosophila melanogaster* acetyl-CoA-carboxylase sustains a fatty acid-dependent remote signal to waterproof the respiratory system. *PLoS Genet.* **8**, e1002925. <https://doi.org/10.1371/journal.pgen.1002925> (2012).
24. Brock, T. J., Browse, J. & Watts, J. L. Fatty acid desaturation and the regulation of adiposity in *Caenorhabditis elegans*. *Genetics* **176**, 865–875. <https://doi.org/10.1534/genetics.107.071860> (2007).
25. Li, Y. & Paik, Y.-K. A potential role for fatty acid biosynthesis genes during molting and cuticle formation in *Caenorhabditis elegans*. *BMB Rep.* **44**, 285–290. <https://doi.org/10.5483/BMBRep.2011.44.4.285> (2011).
26. Tehlivets, O., Scheuringer, K. & Kohlwein, S. D. Fatty acid synthesis and elongation in yeast. *Biochim. Biophys. Acta* **1771**, 255–270. <https://doi.org/10.1016/j.bbali.2006.07.004> (2007).
27. Marza, E., Simonsen, K. T., Faergeman, N. J. & Lesa, G. M. Expression of ceramide glucosyltransferases, which are essential for glycosphingolipid synthesis, is only required in a small subset of *C. elegans* cells. *J. Cell Sci.* **122**, 822–833. <https://doi.org/10.1242/jcs.042754> (2009).
28. Savage, D. B. *et al.* Reversal of diet-induced hepatic steatosis and hepatic insulin resistance by antisense oligonucleotide inhibitors of acetyl-CoA carboxylases 1 and 2. *J. Clin. Invest.* **116**, 817–824. <https://doi.org/10.1172/JCI27300> (2006).
29. Beckers, A. *et al.* Chemical inhibition of acetyl-CoA carboxylase induces growth arrest and cytotoxicity selectively in cancer cells. *Cancer Res.* **67**, 8180–8187. <https://doi.org/10.1158/0008-5472.CAN-07-0389> (2007).
30. Stiernagle, T. Maintenance of *C. elegans*. *WormBook: The Online Review of C. elegans Biology*, 1–11. <https://doi.org/10.1895/wormbook.1.101.1> (2006).
31. Barros, A. G. D. A., Liu, J., Lemieux, G. A., Mullaney, B. C. & Ashrafi, K. Analyses of *C. elegans* fat metabolic pathways. *Methods Cell Biol.* **107**, 383–407. <https://doi.org/10.1016/B978-0-12-394620-1.00013-8> (2012).
32. vom Dorp, K., Dombrink, I. & Dörmann, P. Quantification of diacylglycerol by mass spectrometry. *Methods Mol. Biol. (Clifton, N.J.)* **1009**, 43–54. https://doi.org/10.1007/978-1-62703-401-2_5 (2013).
33. Schöning, R. Residue analytic method for the determination of residues of spirotetramat and its metabolites in plant and on plant material by HPLC-MS/MS. *Bayer CropSci. J.* **61**, 417–453 (2008).
34. Ren, J. *et al.* DOG 1.0: illustrator of protein domain structures. *Cell Res.* **19**, 271–273. <https://doi.org/10.1038/cr.2009.6> (2009).
35. Saitou, N. & Nei, M. The neighbor-joining method: a new method for reconstructing phylogenetic trees. *Mol. Biol. Evol.* **4**, 406–425. <https://doi.org/10.1093/oxfordjournals.molbev.a040454> (1987).
36. Felsenstein, J. Confidence limits on phylogenies: an approach using the bootstrap. *Evol. Int. J. Org. Evol.* **39**, 783–791. <https://doi.org/10.1111/j.1558-5646.1985.tb00420.x> (1985).
37. Nei, M. & Kumar, S. *Molecular Evolution and Phylogenetics* (Oxford University Press, New York, 2000).
38. Tamura, K. *et al.* MEGA5: molecular evolutionary genetics analysis using maximum likelihood, evolutionary distance, and maximum parsimony methods. *Mol. Biol. Evol.* **28**, 2731–2739. <https://doi.org/10.1093/molbev/msr121> (2011).
39. Sukno, S. A. *et al.* Quantitative detection of double-stranded RNA-mediated gene silencing of parasitism genes in *Heterodera glycines*. *J. Nematol.* **39**, 145–152 (2007).
40. Patel, N. *et al.* A nematode effector protein similar to annexins in host plants. *J. Exp. Bot.* **61**, 235–248. <https://doi.org/10.1093/jxb/erp293> (2010).
41. Schmittgen, T. D. & Livak, K. J. Analyzing real-time PCR data by the comparative C(T) method. *Nat. Protoc.* **3**, 1101–1108. <https://doi.org/10.1038/nprot.2008.73> (2008).

Acknowledgements

Open access funding provided by Projekt DEAL.

Author contributions

P.G. and F.M.W.G. conceived and designed the research. P.G. and K.G. performed the experiments. A.E. and S.S. conducted data analysis. P.G. drafted the manuscript. K.G., R.N., S.S., J.B., P.D. and F.M.W.G. reviewed the manuscript.

Competing interests

The authors declare no competing interests.

Additional information

Supplementary information is available for this paper at <https://doi.org/10.1038/s41598-020-69624-5>.

Correspondence and requests for materials should be addressed to F.M.W.G.

Reprints and permissions information is available at www.nature.com/reprints.

Publisher's note Springer Nature remains neutral with regard to jurisdictional claims in published maps and institutional affiliations.



Open Access This article is licensed under a Creative Commons Attribution 4.0 International License, which permits use, sharing, adaptation, distribution and reproduction in any medium or format, as long as you give appropriate credit to the original author(s) and the source, provide a link to the Creative Commons license, and indicate if changes were made. The images or other third party material in this article are included in the article's Creative Commons license, unless indicated otherwise in a credit line to the material. If material is not included in the article's Creative Commons license and your intended use is not permitted by statutory regulation or exceeds the permitted use, you will need to obtain permission directly from the copyright holder. To view a copy of this license, visit <http://creativecommons.org/licenses/by/4.0/>.

© The Author(s) 2020